Archives of Hydro-Engineering and Environmental Mechanics
Vol. 49 (2002), No. 4, pp. 17–35

On the Maximum Horizontal Forces Exerted by Floating Ice on Engineering Structures

Ryszard Staroszczyk

Institute of Hydro-Engineering of the Polish Academy of Sciences,
ul. Waryńskiego 17, 71-310 Szczecin, Poland;
Present address: School of Mathematics, University of East Anglia, Norwich NR4 7TJ,
United Kingdom, e-mail: r.staroszczyk@uea.ac.uk

(Received April 5, 2002; revised October 15, 2002)

Abstract. The paper concerns the problem of calculation of the maximum horizontal forces that a floating ice cover can exert on isolated, vertical-walled, engineering structures. The analysis is carried out on the assumption that the largest possible force which can occur in a floating ice plate is determined by the elastic buckling failure mechanism. Hence, the buckling loads of a semi-infinite, wedge-shaped in-plane, thin elastic plate resting on a liquid base and pressing against a rigid structure of a limited width are evaluated. The problem is solved by applying the finite-element method. The results of numerical calculations illustrate the variation of the buckling force with the thickness of ice, the width of the structure, the angle defining the in-plane shape of the plate, and the type of boundary conditions at the ice–structure contact zone. The comparison of the results obtained in this work with those given by approximate analytic estimates available in literature, has shown that the latter considerably overestimate the bearing capacity of ice, therefore new relations are proposed in this paper.

Notations

$b(x)$	plate width at x,
b_0	structure width,
D	plate flexural rigidity,
E	Young's modulus of elasticity,
g	acceleration due to gravity,
h	plate thickness,
M	bending moment per unit width of a plate,
N	normal tensile force per unit width of a plate,
n	ice porosity,
P	total compressive force in a plate cross-section,
P_0	buckling force for a plate of uniform width,

Q	shear force per unit width of a plate,
q	distributed load intensity,
T	ice temperature,
w	plate deflection,
x, y, z	rectangular Cartesian coordinates,
z_0	plate neutral plane position,
α	wedge angle,
$\epsilon_{xx}, \epsilon_{yy}$	infinitesimal strain tensor components,
κ	curvature of a plate deflection curve,
ν	Poisson's ratio,
ϱ	water density,
σ_{xx}, σ_{yy}	Cauchy stress tensor components.

1. Introduction

Ice cover which is formed on the free surface of freezing sea, lake, or river water is capable of exerting large-magnitude forces on engineering structures, such as dams, breakwaters, bridge piers, or legs of off-shore oil drilling platforms. Since the ice forces acting on a structure result from the wind and water current action, as well as ice thermal expansion, all taking place over areas exceeding many times the dimensions of the structure itself, their net effect on the structure can be significant. Therefore, for the structure failure risk assessment, the proper calculation of loads exerted by a floating ice cover is of prime importance. In this work we focus on the determination of the *maximum horizontal forces* to which a structure can be subjected due to the action of a floating ice sheet.

It is well known that ice is a highly creeping material, in which, under typical loading conditions, creep deformations relatively quickly (in a matter of minutes) overtake elastic strains (Mellor 1980, Sanderson 1988, Staroszczyk 2001). Because of the viscoelastic, rather than purely elastic, behaviour of ice, the failure mode which is most commonly observed in relatively thin (up to ~ 0.5 m thick) floating ice sheets during ice – structure interaction events is that of creep buckling. Usually, creep buckles develop in ice over periods ranging from several hours to several days, during which the ice deformations grow steadily with time. Also, the contact forces exerted on a structure by the floating ice vary with time, depending on the current and past loading. The magnitudes of these contact forces, however, are bounded by either a force which leads to the purely elastic buckling of the ice plate, or a force which gives rise to crushing (brittle fracture) of ice, whichever of the two is smaller in magnitude. For this reason, even though purely elastic buckling modes are rarely observed in the field, we are concerned here with the elastic buckling forces alone, since these forces, as the largest possible forces acting on the structure, determine the design loads for an engineer. Such an approach not

only simplifies the analysis, but also gives us the certainty that we are on the safe side when designing a structure.

The considerations are carried out on the assumption that the behaviour of an ice cover can be approximated by that of an elastic plate floating on a liquid base, and the standard theory of elastic plates can be applied. The floating plate is bent by the lateral (vertical) loads caused by the elastic reaction of the underlying water, and is also subjected to in-plane compression due to the action of wind and water currents pushing the plate towards an engineering structure. The structure is supposed to be a rigid and vertical wall of finite length, and is treated as an isolated structure, that is no interaction between a group of structures and the floating plate is considered. The floating plate is assumed to be of uniform thickness, with the elastic properties varying with depth to account for the possible nonhomogeneity of the ice due to the presence of pores in the material. In the horizontal plane, the floating plate is supposed to have the shape of a truncated wedge of semi-infinite length. Such a geometry is adopted in order to reflect realistic conditions occurring in the field, in which, at sufficiently large loads, radial cracks emanating from the edges of the structure usually develop in the ice plate, thus bounding the domain of the cover that is involved in the interaction with the structure (Sanderson 1988).

The problem of calculating the buckling forces in a wedge-shaped elastic plate on an elastic foundation has already been considered in a number of papers, see, for instance (Kerr 1978, Nevel 1980 and Sanderson 1988), in which approximate estimates, obtained analytically, are given. Some relevant analytical results can also be found in (Kerr, Palmer 1972), and some experimental data on elastic buckling of ice have been reported by (Sodhi et al. 1983). In this work the problem under investigation is solved by using the finite-element method. Assuming that the forces driving the plate towards the rigid wall act in the direction normal to the wall, the elastic buckling forces are determined as a function of the structure width, ice thickness, the angle defining the plate shape, and the type of boundary conditions at the contact zone. The results obtained are compared with those predicted by approximate solutions given by (Kerr 1978), and subsequently reproduced by (Sanderson 1988). It turns out that the results given by the latter authors lead to a significant overestimation of the buckling forces that a wedge-shaped elastic plate can sustain, and some inconsistency in the analytical results by (Kerr 1978) also exists. Therefore, by fitting to our numerical results, new approximate formulae for determining the buckling forces in floating wedge-shaped elastic plates are proposed.

2. Formulation of the Problem

When a coherent floating ice cover is pressed, as a result of wind and current forces, against a flat structure of limited width, at a certain magnitude of load-

ing, radial cracks usually form in ice near the vertical edges and subsequently propagate through the cover. Such a phenomenon, observed in both laboratory tests and in the field (Kerr 1978, Sanderson 1988), leads to the separation of a wedge-shaped plate, shown in Fig. 1a, which interacts with the structure, while the other part of the cover no exerts practically loads on the structure. We idealise the problem by supposing that the wedge is symmetric around the x-axis, its geometry described by the structure width b_0 and the angle α, and the ice cover extends to infinity. We further assume that the action of wind and water currents is such that the plate is pushed towards the structure, modelled as a rigid, vertical wall, in the direction normal to the structure face, i.e. in the direction of negative x. The plate is assumed to be of a uniform thickness, denoted by h (see Fig. 1b), and the ice sheet in perfect contact with the underlying water, i.e. no lift-off of the plate occurs. Since the elastic properties of floating ice, and in particular sea ice, can vary significantly with depth due to variation of ice temperature and porosity, we assume that the Young modulus changes through the depth of the ice cover. Our aim is to determine the magnitude of a compressive force in the ice at which the wedge-shaped plate buckles in an elastic manner.

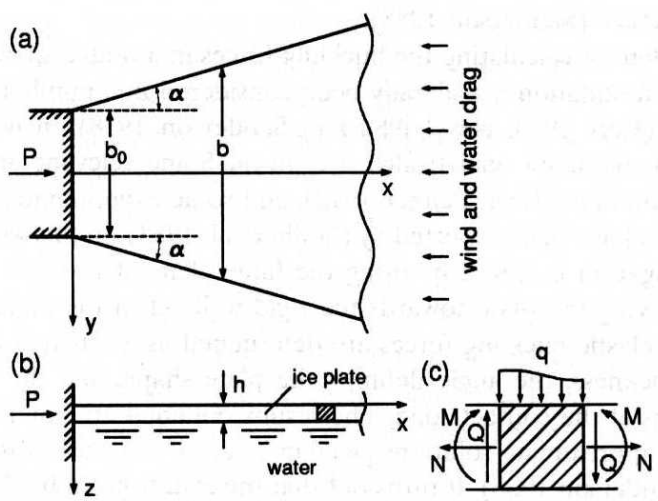

Fig. 1. Geometry of a wedge-shaped plate of floating ice interacting with a rigid structure of the width b_0: (a) plane view, (b) plate cross-section, (c) definition of internal forces

In order to solve the problem, we apply the classical, linear theory of thin elastic plates (Timoshenko, Woinowsky-Krieger 1959), based on the assumptions that (1) the plate deflections are small (that is of the order of its thickness), (2) the ratio of the deflection to a characteristic length (here the half-wavelength of elastic buckles) is small too, (3) the effects due to shear stresses are neglected, so (4) the plate cross-sections which are normal to the middle plane before bending remain

plane and normal to the middle surface during deformation (the Bernoulli-Euler assumption), and (5) the normal stresses in the direction transverse to the plate are disregarded. In our case, the plate is bent by the lateral loads caused by the elastic reaction of the liquid base when the ice cover is either lifted or depressed from its floating equilibrium state, with the magnitude of the restoring force proportional to the plate deflection. Besides the bending, the plate is also under the action of compressive stresses along the x-axis, coming from the wind and water drag forces at the upper and lower plate surfaces.

We adopt the z coordinate axis directed downwards, as shown in Fig. 1b, with the upper face of the plate at $z = 0$, and the lower face at $z = h$. The plate deflection along the z-axis is denoted by w, and the plate internal forces per unit length: the bending moment M, the vertical shear force Q, and the normal (tensile) force N, are all defined in Fig. 1c. Neglecting the body forces (e.g. the own weight) in the plate, and considering the equilibrium of forces in the z-axis direction as well as the bending moments acting on an infinitesimal element of the plate cut by a pair of planes parallel to the yz coordinate planes, we obtain the following differential equations:

$$\frac{dQ}{dx} + N\frac{d^2w}{dx^2} = -q, \qquad \frac{dM}{dx} = Q, \tag{1}$$

where q is the lateral distributed load acting along the z-axis. By eliminating the shear force Q between the two latter equations, we obtain the relation

$$\frac{d^2M}{dx^2} + N\frac{d^2w}{dx^2} = -q. \tag{2}$$

We assume that the only lateral load which is exerted on the plate is that of the elastic reaction of the underlying water. Adopting the Winkler-Zimmerman assumption that the plate deflection w at any point is proportional to the foundation pressure p at that point, and does not depend on the pressure at any other point of the foundation, the load q is expressed by

$$q = -\varrho g w, \tag{3}$$

where ϱ is the water density and g the acceleration due to gravity. We further assume that, due to the symmetry of the problem about the x-axis, the plate displacement w and all the loads acting on the plate are the function of x only, that is $w = w(x)$, $M = M(x)$, $q = q(x)$, etc., and there is no bending of the plate in the direction of the y-axis, i.e. that the plate is bent cylindrically in the plane xz. Hence, in fact, we reduce the problem to that of a beam of variable cross-section resting on an elastic foundation and subjected to bending and compression (retaining, however, the dependence of flexural rigidity on the Poisson ratio, in a form characteristic of plates). Although the assumption introduced above is a

considerable simplification, it is believed that the results obtained, at least for small wedge angles α, will not differ significantly from those obtained by solving a full two-dimensional plate problem, and therefore will be useful in engineering practice.

In order to relate the bending moment $M(x)$ to the plate deflection $w(x)$, we employ the standard methods of the classical theory of thin plates, which we now summarise in brief. Due to the nonuniformity of the plate, resulting from the variation of the Young modulus with depth, we should account for the fact that the neutral plane does not coincide with the middle plane which is defined, in undeformed state, by $z = h/2$. However, we still adopt the plane cross-section assumption, which implies a linear variation of normal strains $\epsilon_{xx}(x, z)$ and $\epsilon_{yy}(x, z)$ in the plate. Hence, denoting the location of the neutral plane by z_0, and assuming that the normal strains in the yz cross-section are proportional to the curvature κ of the deformed plate, we can express ϵ_{xx} by means of the relation

$$\epsilon_{xx} = \kappa(z - z_0). \tag{4}$$

By virtue of Hooke's law, the normal strains ϵ_{xx} and ϵ_{yy} are given by

$$\epsilon_{xx} = \frac{\sigma_{xx}}{E} - \frac{\nu\sigma_{yy}}{E}, \qquad \epsilon_{yy} = \frac{\sigma_{yy}}{E} - \frac{\nu\sigma_{xx}}{E}, \tag{5}$$

where σ_{xx} and σ_{yy} denote the normal stresses, E is Young's modulus, and ν is Poisson's ratio. Since the lateral strain in the y direction has to be zero to maintain the plate continuity during bending, that is $\epsilon_{yy} = 0$, we obtain from equations (4) and (5) the relation for the normal stress in the x direction in the form:

$$\sigma_{xx} = \frac{E\kappa(z - z_0)}{1 - \nu^2}, \tag{6}$$

which indicates that the normal stress distribution is not linear in the z direction as E is a function of z. The bending moment $M(x)$ per unit width of the plate is determined by integrating the normal stress σ_{xx} over the plate cross-section, that is

$$M = \int_0^h \sigma_{xx}(z - z_0)\mathrm{d}z, \tag{7}$$

which, after substituting (6), yields the expression

$$M = \frac{\kappa}{1 - \nu^2} \int_0^h (z - z_0)^2 E(z)\mathrm{d}z = \kappa D, \tag{8}$$

in which D is the flexural rigidity of the plate defined by

$$D = \frac{1}{1 - \nu^2} \int_0^h (z - z_0)^2 E(z)\mathrm{d}z. \tag{9}$$

The location of the neutral plane is determined from the condition that the resultant normal force due to bending, obtained by integrating the stress σ_{xx} over $0 \leq z \leq h$, is zero, which, in view of (6), yields

$$\int_0^h (z - z_0)\, E(z) \mathrm{d}z = 0. \tag{10}$$

Now, assuming that the plate displacement w is small enough to make $(dw/dx)^2 \ll 1$, we can express the curvature (considered positive if it is convex downward) in terms of the plate deflection by means of $\kappa = -d^2w/dx^2$. By substituting first the latter relation for κ into (8), and then (8) and (3) into (2), we arrive at the following differential equation

$$D\frac{d^4w}{dx^4} - N\frac{d^2w}{dx^2} + \varrho g w = 0. \tag{11}$$

The latter relation describes the behaviour of the plate of a unit width. To derive the relation for the wedge-shaped plate, we multiply both sides of (11) by the plate width $b(x)$, defined by

$$b(x) = b_0 + 2x \tan\alpha, \tag{12}$$

to obtain the following equation for an elastic plate on a liquid base subjected to the combined action of bending and axial compression:

$$Db(x)\frac{d^4w}{dx^4} + P\frac{d^2w}{dx^2} + \varrho g b(x) w = 0, \quad 0 < x < \infty. \tag{13}$$

In (13), $P = -Nb$ is the total compressive load carried through the whole cross-section b of the wedge. The load P is assumed to be independent of x in the region adjacent to the structure located at $x = 0$, that is, in the region where, for $\alpha > 0$, elastic buckling is expected to occur. Such an approximation seems to be permitted, since a typical magnitude of the buckling force is much larger than the resultant tangential load due to wind and current drags acting over a relatively small area of ice cover in the vicinity of the structure.

The differential equation (13) is solved with two types of boundary conditions at the ice–structure contact area. The first type describes the case of a simply-supported edge of the plate, with zero deflection and bending moment at $x = 0$, while the other corresponds to the case of a rigidly-supported (clamped) end, with zero deflection and slope at $x = 0$. According to Sanderson 1988, the first case is more realistic in practice, as perfect adfreezing between ice and a structure is rarely observed in the field. These two types of boundary conditions are expressed, respectively, by

$$w(0) = 0, \qquad \frac{d^2w}{dx^2}(0) = 0, \tag{14}$$

$$w(0) = 0, \qquad \frac{dw}{dx}(0) = 0. \tag{15}$$

Apart from the conditions (14) and (15), the regularity conditions are to be satisfied at $x \to \infty$.

The variation of Young's modulus E with depth is primarily caused by the change of ice temperature and porosity across an ice cover, which may result in a substantial reduction of E in the warmer, and usually more porous, lower layers of an ice plate. In the case of ice sheets thicker than about 0.5 m, the modulus E also varies due to the presence of different types of ice — typically ice in the upper layer is isotropic, while that in the lower layer is anisotropic. In this work we restrict our attention to plates of thicknesses not exceeding 0.5 m (since for thicker plates the elastic buckling mechanism plays no practical role), and therefore we consider only isotropic ice. For such ice, the dependence of the Young modulus on temperature T can be described by the relation given by (Sinha 1989)

$$E(T) = 8.93 + 1.2 \times 10^{-2}(T_m - T) \quad \text{[GPa]}, \tag{16}$$

where T_m is the ice melting temperature. Slightly different relations describing the variation of E with T have been proposed by (Hutter 1983 and Nanthikesan, Sunder 1994).

The porosity of floating ice is mainly due to the formation and subsequent development of pockets of a solution of salt and water. The latter process, in which the brine pockets migrate through the ice cover in the direction of temperature gradients, is of a thermodynamic nature (Schwarz, Weeks 1977, Sanderson 1988, Staroszczyk 2001) and requires sufficient time, measured in weeks and months, to develop. For this reason, the process is of little importance in the case of thin (that is young) ice. On the other hand, its role significantly increases with the increase of ice thickness, and in sufficiently old ice sheets, depending on temperature and the salinity of sea water, the porosity of ice due to brine content can well exceed 10% (Sanderson 1988). Experimental evidence proves that the effect of ice porosity on Young's modulus is pronounced. (Hutter 1983) has suggested the following fit to empirical data to describe the weakening of ice with its porosity:

$$\frac{E(n)}{E_T} = \begin{cases} 1 - 5n, & 0 \le n < 0.15, \\ 47.168(0.15 - n)^3 - 45.97(0.15 - n)^2 + \\ \quad + 0.5(0.15 - n) + 0.25, & 0.15 \le n < 0.4, \\ 0.06(1 - n), & 0.4 \le n \le 1, \end{cases} \tag{17}$$

where n denotes porosity and E_T is the value of Young's modulus for pure (bubble-free) ice at a given temperature. It follows from (17) that, for example, 10% ($n = 0.1$) volume porosity of isotropic ice leads to a 50% reduction of the elastic modulus.

Contrary to the Young modulus, the Poisson ratio ν is much less sensitive to ice temperature and porosity. Its temperature dependence can be approximated by the relation proposed by (Sinha 1989)

$$\nu(T) = 0.308 + 7 \times 10^{-5}(T_m - T). \tag{18}$$

There is some variation of ν with the porosity of ice, but (Hutter 1975) has demonstrated that in typical sea ice problems this variation can be ignored, and hence a constant value of the Poisson ratio can be applied.

Due to rather small thicknesses of ice plates considered in this analysis, it seems justified to assume for practical purposes a linear variation of Young's modulus with the depth of ice. Denote the value of the elastic modulus E at the upper surface of the plate ($z = 0$) by E_0, and that at the lower surface ($z = h$) by βE_0, where $0 \leq \beta \leq 1$. Then, with the linear variation of $E(z)$ between the two values, the relation (10) determines the position of the neutral plane z_0 by

$$z_0 = h \frac{1 + 2\beta}{3(1 + \beta)}, \tag{19}$$

which, obviously, yields for $\beta = 1$ (E is constant across the plate) the value $z_0 = h/2$, meaning that the neutral plane coincides with the middle plane. With z_0 given by (19), the relation (9) defines the plate flexural rigidity by

$$D = \frac{E_0 h^3}{12(1 - \nu^2)} \left[\frac{1 + 4\beta + \beta^2}{3(1 + \beta)} \right]. \tag{20}$$

For the particular case of $\beta = 1$, the term in the square brackets becomes unity, hence the expression for the rigidity reduces to that for a homogeneous plate, $D = E_0 h^3/[12(1 - \nu^2)]$. For $\beta = 0.5$ (the modulus at the top of the plate is twice as high as at the bottom) the rigidity reduces to about 0.72 of that of a homogeneous plate, while for the limit case $\beta = 0$ the plate rigidity decreases to 1/3 of that for uniform pure ice.

3. Solution of the Problem

The fourth-order differential equation (13), supplemented by the appropriate boundary conditions, either (14) or (15), describes the eigenvalue problem from which the buckling force P can be determined. Because of the presence of the variable coefficient $b(x)$ in (13), no exact closed-form of analytical solution is available for the general case of a wedge-shaped plate defined by $\alpha > 0$. However, in the particular case of $\alpha = 0$, corresponding to the case of a parallel-sided plate with $b(x) = b_0$, equation (13) reduces to the equation with constant coefficients, for which an analytical solution can be obtained in a straightforward manner, and has the form

$$P_0 = 2b_0\sqrt{\varrho g D}, \tag{21}$$

valid for both simply-supported and clamped boundary conditions at $x = 0$ (Kerr 1978). An approximate, semi-analytical solution of equation (13) for the general case of $\alpha > 0$ was constructed by (Kerr 1978) who obtained, for the boundary conditions (14) and (15) for a simply-supported and a clamped plate end, the following two relations respectively:

$$\text{simply-supported end:} \qquad P = c_1 \mu D\,(\mu b_0 + 2\tan\alpha), \tag{22}$$

$$\text{rigidly-supported end:} \qquad P = c_2 \mu D\,(2\mu b_0 + 2\tan\alpha), \tag{23}$$

with

$$\mu^4 = \frac{\varrho g}{4D}, \tag{24}$$

and the constants $c_1 = 5.3$ and $c_2 = 8$. The same relations were subsequently repeated in the book by Sanderson 1988. We immediately observe, however, that the above two approximate results are inconsistent with the relation (21), as they yield for the wedge angle $\alpha = 0$ the values of the buckling forces P for a parallel-sided plate which: (1) are different for both types of boundary conditions at $x = 0$, whereas they should be identical, and (2) neither of them equals the value given by (21), since (22) supplies $P = 2.65\, b_0(\varrho g D)^{1/2}$, and (23) leads to $P = 8\, b_0(\varrho g D)^{1/2}$. Thus the approximations (22) and (23) are apparently erroneous, and for this reason we solve the problem under consideration by employing a discrete method in order to explore in detail the quantitative features of the behaviour of a plate subjected to elastic buckling, and, on the basis of the results obtained, to formulate in Section 5 new approximate relations that can be useful for an engineer.

The eigenvalue problem defined by equations (13)–(15) can be solved by a number of discrete methods. For instance, by applying the finite-difference method. In such a case, however, the discretisation of the problem leads to the solution of a generalised eigenvalue problem for nonsymmetric matrices, which is much more difficult to solve than that involving symmetric matrices. Therefore, we use here the finite-element method, in which case all the matrices resulting from the discretisation of the problem given by (13) are symmetric, which leads to a significant simplification of the numerics involved in the solution process.

We employ the weighted residual, or Galerkin, method (Zienkiewicz, Taylor 1989), in which the problem equation is satisfied in an integral mean sense. Following this method, the plate is discretised along the x-axis by introducing one-dimensional finite elements. To ensure that both the plate deflection and its slope are continuous between elements, at each nodal point two parameters are used to describe the plate deformations, namely w and dw/dx at that discrete point. Assuming that a given finite element is defined by nodes i and j, located at x_i and x_j, respectively, we approximate the continuous function $w(x)$ within the element ij by means of four interpolation (shape) functions $\Phi_r(x)$ $(r = 1, \ldots, 4)$ as follows:

$$w(x) = w_i \Phi_1 + \theta_i \Phi_2 + w_j \Phi_3 + \theta_j \Phi_4, \tag{25}$$

where $\theta_i = (dw/dx)_i$ and $\theta_j = (dw/dx)_j$ are the nodal values of the plate slope. Introducing a dimensionless coordinate ξ defined by

$$\xi = \frac{x - x_c}{a}, \quad x_c = \frac{x_i + x_j}{2}, \quad -1 \le \xi \le 1, \tag{26}$$

where $2a$ is the length of the element ij, the adopted shape functions are given by

$$\begin{aligned} \Phi_1 &= \tfrac{1}{4}(\xi - 1)^2(2 + \xi), & \Phi_3 &= \tfrac{1}{4}(\xi + 1)^2(2 - \xi), \\ \Phi_2 &= \tfrac{a}{4}(\xi - 1)^2(\xi + 1), & \Phi_4 &= \tfrac{a}{4}(\xi + 1)^2(\xi - 1). \end{aligned} \tag{27}$$

By multiplying equation (13), in turn, by a set of weighting functions, which in the Galerkin method are identical with the interpolation functions Φ_s, and then integrating the resulting relations over the plate length $x \ge 0$ and applying in the process Green's theorem to reduce the order of differentiation, we obtain a system of $2N$ linear algebraic equations, with N being the number of nodes, which can be written as

$$(\mathbf{K} + P\mathbf{B} + \mathbf{C})\,\mathbf{w} = \mathbf{O}, \tag{28}$$

where the vector $\mathbf{w} = (w_1, \theta_1, \ldots, w_i, \theta_i, w_j, \theta_j, \ldots, w_N, \theta_N)^T$ contains the values of the plate deflections and slopes at all nodal points of the discrete system. The plate stiffness matrix $\mathbf{K}$ and the matrices $\mathbf{B}$ and $\mathbf{C}$ are aggregated from the respective element matrices $\mathbf{K}^e$, $\mathbf{B}^e$ and $\mathbf{C}^e$ in a way typical of the finite-element method (Zienkiewicz, Taylor 1989). The element matrices, each of the dimension 4×4, have the entries defined for the element ij by the following integrals:

$$\begin{aligned} K^e_{rs} &= D \int_{x_i}^{x_j} b(x) \frac{d^2\Phi_r}{dx^2} \frac{d^2\Phi_s}{dx^2} dx, \quad B^e_{rs} = \int_{x_i}^{x_j} \Phi_r \frac{d^2\Phi_s}{dx^2} dx, \\ C^e_{rs} &= \varrho g \int_{x_i}^{x_j} b(x) \Phi_r \Phi_s dx, \end{aligned} \tag{29}$$

where $r, s = 1, \ldots, 4$, and the functions involved are given by (27).

Equation (28) defines a generalised eigenvalue problem from which the value of the buckling force P, the lowest eigenvalue of the problem, can be calculated together with the associated eigenvector $\mathbf{w}$. To accomplish this, the matrix $\mathbf{B}$ is first decomposed into a product of the lower and upper triangular matrices by using the Cholesky method, and then, by matrix inversions and multiplications, the general eigenvalue problem is reduced into a standard eigenvalue problem for a real and symmetric matrix, subsequently solved by applying the Householder transformation and the QL algorithm.

4. Numerical Results

In numerical computations, 200 finite elements of the same length for plates thinner than $h = 0.2$ m, and 100 otherwise, were used, and the element length was assumed to be equal to $3h$. This means that the length of the plate adopted to approximate the behaviour of a semi-infinite plate was equal to either $600h$ or $300h$. The material constants were taken to be those pertinent to ice at a temperature of $-5°C$, that is, on account of (16) and (18), equal to $E = 8.99$ GPa and $\nu = 0.308$. The water density was assumed to be $\varrho = 10^3$ kgm^{-3}, and $g = 9.81$ ms^{-2}.

The results of numerical calculations illustrating the dependence of the elastic buckling load P on the ice cover thickness h and the angle α defining the shape of the truncated wedge, in the case of a structure of the width $b_0 = 10$ m, are presented in Fig. 2. The solid lines in the figure show the results obtained for a simply-supported edge of the plate at $x = 0$, and the dashed lines correspond to the case of a rigidly-supported edge. The labels by the curves indicate the ice cover thickness in metres. The values of the buckling forces are normalised by the magnitude of the load P_0 causing the buckling of a parallel-sided plate of the width b_0 and the respective thickness h, defined by equation (21), that is the ratios P/P_0 are plotted in the graph.

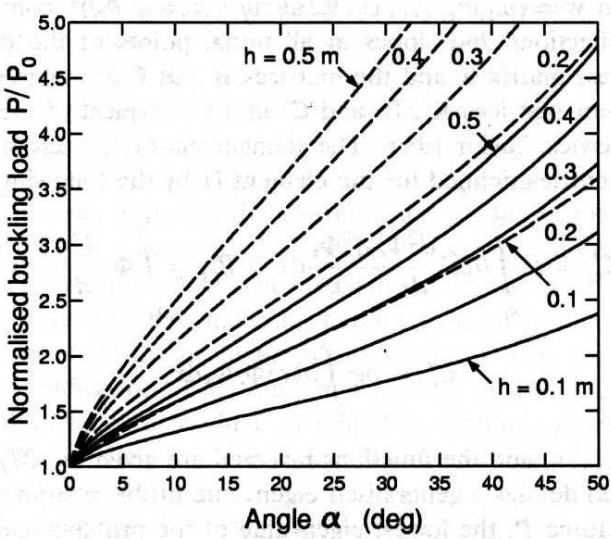

Fig. 2. Variation of the normalised buckling load P/P_0 with the wedge angle α and the ice plate thickness h for simply-supported (solid lines) and rigidly-supported (dashed lines) edge conditions at $x = 0$, for the structure width $b_0 = 10$ m

Corresponding to the previous diagram is Fig. 3, showing the variation of the normalised buckling load P/P_0 with the structure width b_0 and the wedge

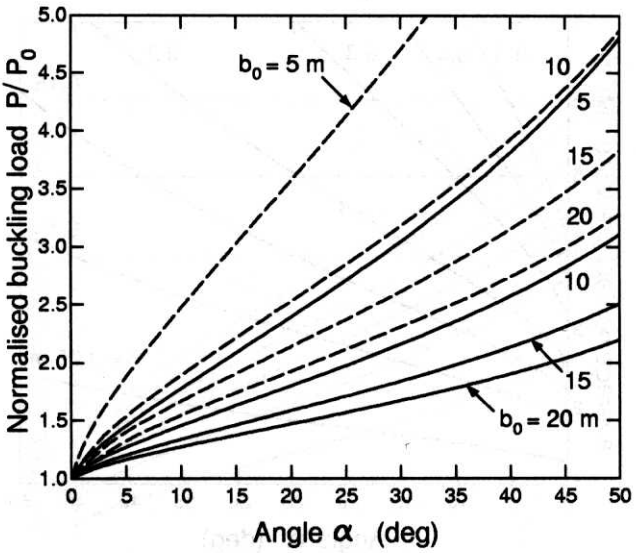

Fig. 3. Variation of the normalised buckling load P/P_0 with the wedge angle α and the structure width b_0 for simply-supported (solid lines) and rigidly-supported (dashed lines) edge conditions at $x = 0$, for the ice plate thickness $h = 0.2$ m

angle α for a fixed ice thickness $h = 0.2$ m. Again, the results obtained for both simply-supported (solid lines) and clamped (dashed lines) plate edge conditions at $x = 0$ are shown. We note an increasing influence of the boundary conditions at $x = 0$ on the buckling force with a decreasing width of the structure.

Fig. 4 presents the average critical buckling pressures, defined by $P/(b_0 h)$, which are exerted by a floating ice cover on a structure 10 m wide. The dependence of these pressures on the plate geometry given by the angle α for different ice thicknesses h is illustrated for a plate which is simply-supported at its edge $x = 0$. A horizontal dashed-dotted line in the figure indicates a pressure level at which ice fails by crushing. Following Sanderson 1988, we assume that this limit value is equal to 5 MPa. Above the latter value, elastic buckling is unlikely to occur since the ice uniaxial crushing strength is exceeded earlier than the level of compressive load P required to buckle the plate is attained. Accordingly, it follows from the figure that only ice plates thinner than about 0.15 m fail by elastic buckling irrespective of the plate geometry (we confine our attention to the angles $\alpha \leq 50°$, as larger values of α seem to be unrealistic, and also because of the simplifications adopted in Section 2). On the other hand, it can be seen in the figure that ice plates thicker than about 0.4 to 0.5 m are most likely to crush before they buckle, even in the case of nearly parallel-sided plates, defined by small values of the wedge angle, say $\alpha \leq 5°$. When the edge of the plate is clamped, rather than simply-supported, then the above limit ice thicknesses h are smaller by a factor of about 1.5.

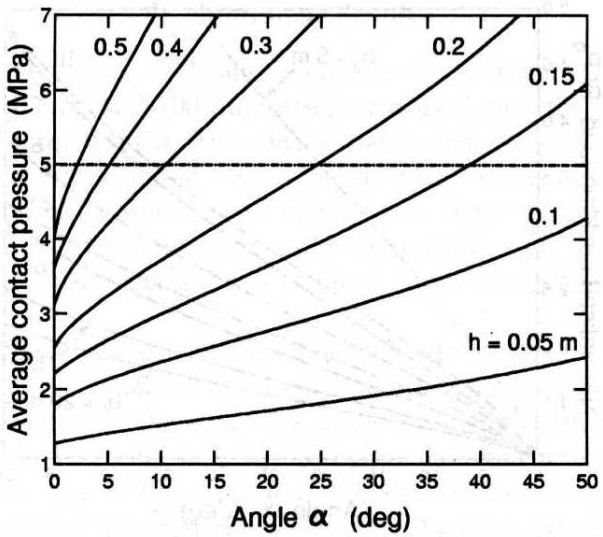

Fig. 4. Variation of the average contact pressure with the angle α and the ice plate thickness h for simply-supported edge conditions at $x = 0$ and the structure width $b_0 = 10$ m. The dashed-dotted line indicates the uniaxial crushing strength of ice

The results presented in Figs. 2–4 have been obtained for uniform ice, with the elastic modulus E assumed to be constant throughout the plate. In Fig. 5 we illustrate the effect of the weakening of ice with increasing depth on the average contact pressures exerted on a structure. The plots, obtained for the fixed ice thickness $h = 0.2$ m and structure width $b_0 = 10$ m, show the variation of the contact pressure $P/(b_0 h)$ with the wedge angle α and parameter β, the latter used to describe a linear change of E from E_0 to βE_0 between the upper and the lower plate surfaces, respectively. For the angle $\alpha = 0$ (parallel-sided plate) the buckling force P, and hence the average contact pressure, is proportional to $\sqrt{D}$, as follows from the relation (21), with D decreasing with decreasing β in the way defined by (20). For larger values of α, the average contact pressures decrease slightly faster than $\sqrt{D}$ decreases.

Fig. 6 illustrates buckling modes for an ice plate of a thickness $h = 0.2$ m and width $b_0 = 10$ m, with simply-supported edge conditions at $x = 0$. The curves depict the plate displacement w for different wedge angles α, given in deg. For a plate of uniform width, defined by $\alpha = 0$, the buckling mode can be determined analytically, and is described by the relation $w(x) = \sin(\lambda x)$, where $\lambda^4 = \varrho g / D = 4\mu^4$. The latter yields the length of the buckling half-wave, given by $L = \pi/\lambda$, to be equal to 16.01 m for the adopted ice thickness h, and we note that the buckling mode for $\alpha = 0$ computed by solving the eigenvalue problem (28) numerically is very close to that determined analytically. We also observe that for wedge angles $\alpha > 0$, even as small as 5°, the deformation of the plate in buckling attenuates

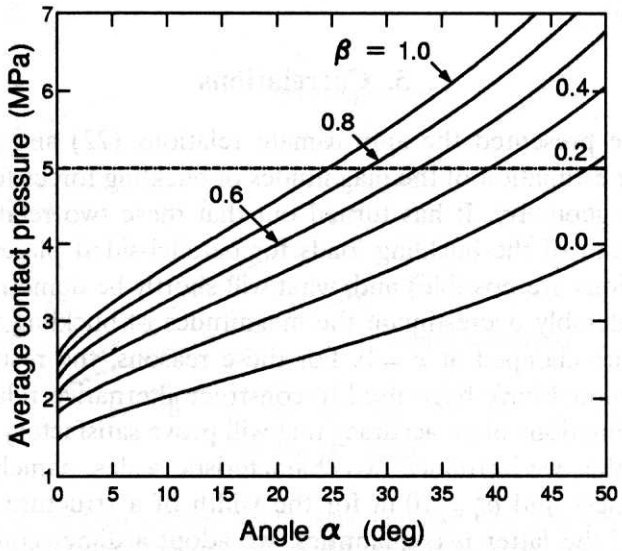

Fig. 5. Variation of the average contact pressure with the angle α and parameter β for plate $h = 0.2$ m thick and $b_0 = 10$ m wide at $x = 0$, with a simply-supported edge. The dashed-dotted line indicates the uniaxial crushing strength of ice

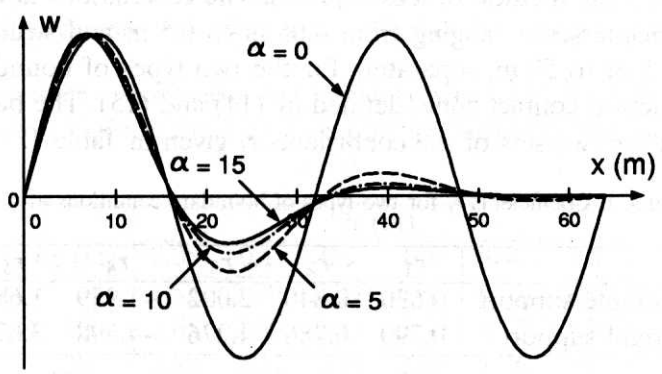

Fig. 6. Buckling modes for various wedge angles α (given in deg), for the plate $h = 0.2$ m thick and $b_0 = 10$ m wide at $x = 0$, with a simply-supported edge

very rapidly with the distance from the structure, thus indicating that only a small region of a wedge-shaped ice plate, adjacent to the edge $x = 0$, is susceptible to elastic buckling.

5. Correlations

In Section 3 we presented the approximate relations (22) and (23), derived by (Kerr 1978), for estimation of the magnitudes of buckling forces for floating plates of a prescribed geometry. It has turned out that these two relations fail to predict correct values of the buckling loads for parallel-sided plates (in which case analytical solutions are possible) and, what will shortly be demonstrated in Fig. 7, they also considerably overestimate the magnitudes of buckling forces, in particular for the plate clamped at $x = 0$. For these reasons, the results given by our finite-element model have been used to construct alternative relations that could provide approximations of an accuracy that will prove satisfactory for an engineer. To accomplish this, we introduce two characteristic scales, namely $h^* = 0.1$ m for the plate thickness and $b_0^* = 10$ m for the width of a structure interacting with ice. In terms of the latter two quantities, we adopt a dimensionless relation for the buckling load P, in the form of the following representation:

$$\frac{P}{P_0} = 1 + \left(\frac{h}{h^*}\right)^{r_1} \left(\frac{b_0}{b_0^*}\right)^{-r_2} \left(r_3\alpha + r_4\alpha^2 + r_5\alpha^3\right), \tag{30}$$

where P_0 is the value of the buckling force for a parallel-sided plate, defined by (21), and r_i ($i = 1, \ldots 5$) are coefficients. The coefficients r_j have been determined by correlating the relation (30) with the results obtained by the finite-element method by using the method of least-squares. The correlations have been carried out for ice thicknesses h ranging from 0.05 m to 0.5 m and structure widths b_0 ranging from 5 m to 50 m, separately for the two types of boundary conditions at the ice–structure contact zone, defined by (14) and (15). The best results were obtained with the two sets of the coefficients r_i given in Table 1.

Table 1. Coefficients r_i for two types of boundary conditions at $x = 0$

	r_1	r_2	r_3	r_4	r_5
simple support	0.630	0.840	2.002	–1.959	1.681
rigid support	0.590	0.786	4.276	–4.698	3.678

As an example, in Fig. 7 we demonstrate the accuracy of the approximate formula (30) with the coefficients r_i listed in Table 1, by comparing the estimations given by (30) (dashed lines) with the results calculated by the finite-element method (solid lines). Dotted lines in the figure show the results predicted by (22) and (23), obtained by (Kerr 1978) and subsequently repeated by Sanderson 1988.

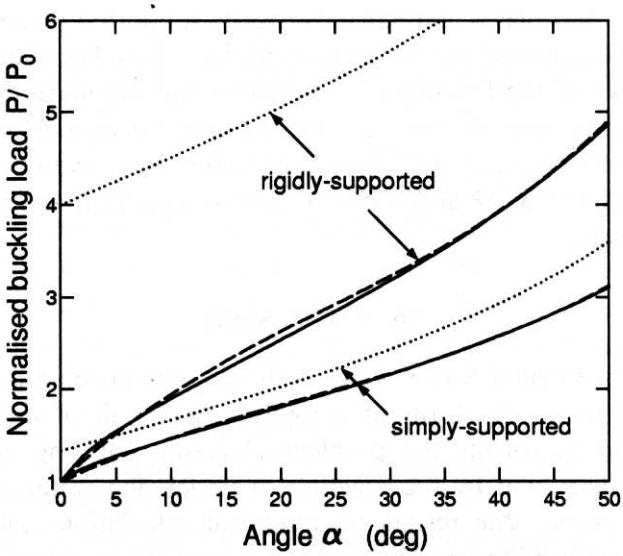

Fig. 7. Comparison of the finite-element results (solid lines) with the estimates given by eq. (30) (dashed lines) for the plate $h = 0.2$ m thick and $b_0 = 10$ m wide, for simply-supported and rigidly-supported edge conditions. Dotted lines show the results predicted by eqs. (22) and (23) proposed by (Kerr 1978)

We see that the latter predictions, given by (22) and (23), differ very substantially from the FEM results. On the other hand, we note a satisfactory agreement between the approximations given by (30) and the "exact" finite-element results, for both simply-supported and clamped plate boundary conditions. For the adopted plate parameters ($h = 0.2$ m and $b_0 = 10$ m), the maximum relative discrepancies between the FEM results and those determined by (30) are equal to 2.8% for the simply-supported plate and 4.0% for the clamped plate.

Table 2. Maximum relative discrepancies (in per cent) between the FEM results and those given by the approximation (30) within the range $0 \leq \alpha \leq 50°$ for plates with simply-supported edges at $x = 0$

	h (m)					
b_0 (m)	0.05	0.1	0.2	0.3	0.4	0.5
5	1.52	2.79	3.74	4.56	6.58	5.81
10	1.65	2.00	2.83	3.60	4.17	3.76
20	2.83	2.35	2.19	2.85	1.76	2.95
50	3.77	3.11	2.84	2.62	1.73	2.19

For other combinations of h and b_0 than that illustrated in the previous figure, and we have explored the ranges $5 \text{ m} \leq b_0 \leq 50$ m, $0.05 \text{ m} \leq h \leq 0.5$ m, and $0° \leq \alpha \leq 50°$, the relative discrepancies are of a similar order, not exceeding 6.6%

for simply-supported plates and 9.5% for rigidly-supported plates. The latter two values have been obtained for the plate width $b_0 = 5$ m. For wider plates, in general, the accuracy of the formula (30) improves and the maximum discrepancies decrease, as can be seen in Table 2. For instance, for $b_0 = 50$ m, the maximum relative differences between the FEM results and those given by the approximation (30) are equal to 3.8% and 5.7% for simply-supported and rigidly-supported plates, respectively.

6. Conclusions

The maximum horizontal forces which a floating ice cover can exert on an engineering structure in the form of a rigid vertical wall of limited width have been determined by solving the problem of elastic buckling of a semi-infinite wedge-shaped plate bent by the reaction of underlying water and subjected to in-plane compression. The results of numerical calculations carried out by the finite-element method illustrate the dependence of the buckling load and the average pressures at the ice–structure contact zone on the shape of the ice cover, its thickness, and a structure size. Due to some simplifying assumptions adopted in the analysis, first of all the reduction of a two-dimensional plate problem to that of a beam of variable cross-section, the results obtained for large wedge angles α should be treated with some caution. Yet, it seems that the results presented in this study can be relied on and applied while assessing a structure failure risk. The comparison of our numerical results with the approximate relations known in the literature has shown that the latter significantly overestimate the bending forces which an ice plate can sustain. For this reason, new approximate relations, derived by the least-squares correlations with the finite-element results, have been proposed. These relations, in the form of simple formulae involving the parameters describing the geometry of an ice plate (its thickness, width at the truncated edge, and the wedge angle) and a set of five parameters for each of the two types of the boundary conditions adopted at the ice-structure interface, provide the estimates which seem to be reasonably accurate, with an error margin of the order of several per cent. Undoubtedly, it would be desirable to compare the calculated buckling forces with laboratory and field measurements. These are, however, very scarce and restricted to laboratory conditions, and the full-scale empirical data for wedge-shaped ice plates are still lacking. Nonetheless, before relevant experimental work has been carried out it is believed that the results obtained in this work are useful for the needs of engineering practice.

Acknowledgement

This work was supported by the Polish Committee for Scientific Research (KBN) under the grant No. 8 T07E 007 20.

References

Hutter K. (1975), Floating sea ice plates and the significance of the dependence of the Poisson ratio on brine content, *Proc. R. Soc. Lond.* A **343** (1632), 85–108.

Hutter K. (1983), *Theoretical Glaciology. Material Science of Ice and the Mechanics of Glaciers and Ice Sheets*, Reidel, Dordrecht.

Kerr A. D. (1978), On the determination of horizontal forces a floating ice plate exerts on a structure, *J. Glaciol.* **20** (82), 123–134.

Kerr A. D., Palmer W. T. (1972), The deformation and stresses in floating ice plates, *Acta Mech.* **15**, 57–72.

Mellor M. (1980), Mechanical properties of polycrystalline ice, In: *Physics and Mechanics of Ice, Proc. IUTAM Symp. Copenhagen 1979* (ed. P. Tryde), pp. 217–245, Springer, Berlin.

Nanthikesan S., Shyam Sunder S. (1994), Anisotropic elasticity of polycrystalline ice Ih. *Cold. Reg. Sci. Technol.* **22** (2), 149–169.

Nevel D. E. (1980), Bending and buckling of a wedge on an elastic foundation. In: *Physics and Mechanics of Ice, Proc. IUTAM Symp. Copenhagen 1979* (ed. P. Tryde), pp. 278–288, Springer, Berlin.

Sanderson T. J. O. (1988), *Ice Mechanics. Risks to Offshore Structures*. Graham and Trotman, London.

Schwarz J., Weeks W. F. (1977), Engineering properties of sea ice. *J. Glaciol.* **19** (81), 499–531.

Sinha N. K. (1989), Elasticity of natural types of polycrystalline ice. *Cold Reg. Sci. Technol.* **17** (2), 127–135.

Sodhi D. S., Haynes F. D., Kato K., Hirayama K. (1983), Experimental determination of the buckling loads of floating ice sheets. *Ann. Glaciol.* **4**, 260–265.

Staroszczyk R. (2001), Mechanical properties of sea ice and their constitutive descriptions, *Arch. Hydroeng. Environ. Mech.* **48** (1), 63–95.

Timoshenko S., Woinowsky-Krieger S. (1959), *Theory of Plates and Shells*. McGraw-Hill, New York, 2nd edn.

Zienkiewicz O. C. and Taylor R. L. (1989), *The Finite Element Method*, vol. 1. McGraw-Hill, London, 4th edn.